

**KAWASAKI STEEL TECHNICAL REPORT**

No.13 ( September 1985 )

---

**Fatigue Properties of 50-kgf/mm<sup>2</sup> High-Strength Hull Structural Steels Manufactured by Thermomechanical Control Process**

Shigeto Matsumoto, Asao Narumoto, Chiaki Shiga, Syuzo Ueda

---

Synopsis :

Fatigue properties of newly developed steels with a tensile strength 50 kgf/mm<sup>2</sup> (490 Mpa) grade, which are manufactured by Kawasaki Thermomechanical Rolling (KTR) and Multipurpose Accelerated Cooling System (MACS), are reported. The newly developed steels exhibit excellent weldability and low-temperature toughness. From the view point of fatigue strength, an investigation has been made on their fatigue properties in the through-thickness direction and on the softening of their high heat input welded joints. The relationship between the through-thickness fatigue strength and sulfur content only was obtained for KTR, MACS and conventional steels. There was no other factor which affects the through-thickness fatigue strength of newly developed steels. Reduction in fatigue strength due to the softening of HAZ was less than 15% when  $K_t$  was 1 and less than 10% when  $K_t$  was 3. Change in the value of  $m$  in Paris' formula due to the softening of HAZ was predicted to be 0.2, which was negligibly small. Base metal and high heat input welded joints of newly developed controlled rolled steels revealed excellent fatigue properties.

(c)JFE Steel Corporation, 2003

**The body can be viewed from the next page.**

# Fatigue Properties of 50-kgf/mm<sup>2</sup> High-Strength Hull Structural Steels Manufactured by Thermomechanical Control Process\*



Shigeto Matsumoto  
Senior Researcher,  
Plate Research Lab.,  
I & S Research Labs.



Asao Narumoto  
Senior Researcher,  
Plate Research Lab.,  
I & S Research Labs.



Chiaki Shiga  
Dr. Engi., Chief of  
Plate Research Lab.,  
I & S Research Labs.



Syuzo Ueda  
Dr. Engi., Chief of  
Lab. II, Mizushima  
Research Dept.,  
I & S Research Labs.

## Synopsis:

Fatigue properties of newly developed steels with a tensile strength 50 kgf/mm<sup>2</sup> (490 MPa) grade, which are manufactured by Kawasaki Thermomechanical Rolling (KTR) and Multipurpose Accelerated Cooling System (MACS), are reported. The newly developed steels exhibit excellent weldability and low-temperature toughness. From the view point of fatigue strength, an investigation has been made on their fatigue properties in the through-thickness direction and on the softening of their high heat input welded joints. The relationship between the through-thickness fatigue strength and sulfur content only was obtained for KTR, MACS and conventional steels. There was no other factor which affects the through-thickness fatigue strength of newly developed steels. Reduction in fatigue strength due to the softening of HAZ was less than 15% when  $K_1$  was 1 and less than 10% when  $K_1$  was 3. Change in the value of  $m$  in Paris' formula due to the softening of HAZ was predicted to be 0.2, which was negligibly small.

Base metal and high heat input welded joints of newly developed controlled rolled steels revealed excellent fatigue properties.

## 1 Introduction

In recent years, 50 kgf/mm<sup>2</sup> (490 MPa) class high-strength steels with a yield point of 32 or 36 kgf/mm<sup>2</sup> (314 or 353 MPa) have been developed with the aid of the thermomechanical control process (TMCP) for use in hull structures. The TMCP is divided into ① the MACS-ACC (Multipurpose accelerated cooling system-accelerated control cooling) process, in which water cooling is conducted following the TMCP, and ②

the KTR (Kawasaki thermomechanical rolling) process, in which rolling is conducted while steel is in the ( $\gamma + \alpha$ ) dual-phase. TMCP steels produced by these methods have high strength, high toughness, and excellent weldability in spite of their low carbon equivalents ( $C_{eq}$ ). From the standpoint of fatigue strength, however, these steels pose the following problems which required examination: ③ Effects of local softening that occurs in the heat-affected zone (HAZ) during a high-heat-input welding and ④ through-thickness fatigue strength. Against this background, an investigation was made into the properties of TMCP steels, such as the fatigue strength of welded joints produced under high-heat-input conditions, and fatigue strength in the through-thickness direction (Z-direction). This paper presents results of this investigation.

\* Originally published in *Kawasaki Steel Giho* 17(1985)1, pp. 73-83

## 2 Materials and Experimental Procedure

### 2.1 Materials

Steels with a yield point of 36-kgf/mm<sup>2</sup> (353 MPa) class produced by the MACS-ACC (hereinafter called MACS) and KTR processes and general hot-rolled steels (conventional steels) of SM50 were used as test materials. **Table 1** and **2** give the chemical compositions and mechanical properties of these steels, respectively. The MACS steels are AH36—25 and 35 mm in thickness, and EH36—38 mm in thickness. The KTR steels are EH36—35 and 38 mm in thickness. The conventional steels are SM50—35 mm in thickness. Through-thickness joints and high-heat-input welded joints were prepared from these steels. **Figure 1** shows the procedure for preparing a through-thickness joint. Steel plates (tab plates) were placed vertically on both sides of the test plate ( $t \times 85 \times 1000$  mm) and submerged arc welding was conducted. **Table 3** shows the high-heat-input welding conditions employed.

### 2.2 Test Specimens

**Figure 2(a)** to **(g)** shows the shapes and dimensions of fatigue test specimens and fatigue crack propagation test specimens. Smooth and notched round-bar specimens used for determining the fatigue strength of the softened part of the HAZ of the joint were prepared in such a manner that the softened part of the HAZ was located at the center of the reduced section. The stress concentration factors were assumed to be 1 (smooth specimen), 1.9, and 3. The following equation<sup>1)</sup> was used for calculating  $K_t$ :

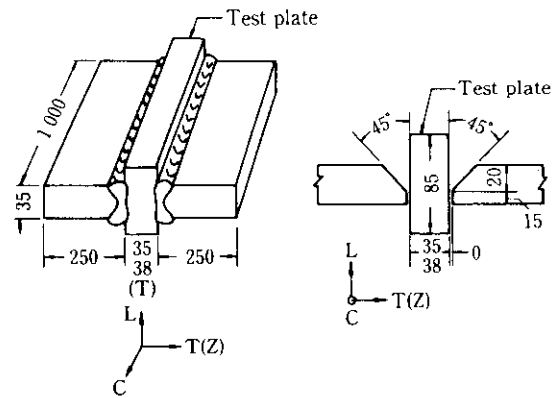


**Fig. 1** Welding procedure of through-thickness direction specimens

$$K_t = 1 + (K_0 - 1) \left\{ 1 - \left( \frac{\theta}{180} \right)^{1+2.4\sqrt{\rho/d}} \right\} \dots (1)$$

where

- $K_t$ : Stress concentration factor for an annular V-notch
- $K_0$ : Stress concentration factor for a semicircular annular notch with a radius of  $\rho$  (according to Peterson's<sup>2)</sup> diagram)
- $\theta$ : Notch angle
- $\rho$ : Notch radius
- $d$ : Notch depth

Center-cracked tension (CCT) specimens and compact type (CT) specimens were used in the fatigue crack propagation test. The notch in welded joint specimens

**Table 1** Chemical composition of materials

(wt %)

Process	Steel	Thickness (mm)	C	Si	Mn	P	S	Al	Cu	Ni	V	$C_{eq}$	$P_{cm}$	
MACS-ACC	M 1	AH36	25	0.17	0.21	0.69	0.012	0.002	0.029	—	—	0.29	0.212	
	M 2		35	0.15	0.24	1.01	0.014	0.003	0.031	—	—	0.32	0.209	
	M 3	EH36	35	0.14	0.25	1.04	0.013	0.003	0.034	—	—	0.31	0.200	
	M 4		38	0.08	0.26	1.48	0.009	0.001	0.039	—	—	0.33	0.163	
KTR	K 1	EH36	38	0.07	0.31	1.56	0.010	0.001	0.028	0.20	0.22	0.037	0.176	
	K 2		35	0.08	0.41	1.50	0.006	0.001	0.030	0.20	0.21	0.036	0.186	
	K 3	35	0.09	0.42	1.50	0.014	0.003	0.032	0.15	0.14	0.042	0.37	0.193	
Conven.	C 1	SM50	35	0.18	0.37	1.36	0.017	0.003	0.033	0.008	0.016	0.003	*0.42	0.261
	C 2			0.16	0.35	1.40	0.017	0.008	0.031	0.009	0.013	0.003	*0.41	0.243

$$C_{eq} = C + Mn/6 + (Cu + Ni)/15 + (Cr + Mo + V)/5 \quad (\%)$$

$$*C_{eq} = C + Mn/6 + Si/24 + Cr/5 + Mo/4 + Ni/40 + V/14 \quad (\%)$$

$$P_{cm} = C + Si/30 + (Mn + Cu + Cr)/20 + Ni/60 + Mo/10 + 5B \quad (\%)$$

**Table 2** Mechanical properties of materials

Process	Steel	Thick-ness (mm)	Direc-tion	YP (kgf/mm <sup>2</sup> )	TS (kgf/mm <sup>2</sup> )	El (%)		
MACS-ACC	M 1	25	L	38	52	35		
			C	39	52	32		
			Z	37	52	—		
	M 2	AH36	35	L	39	56	29	
				C	39	56	28	
				Z	41	55	—	
	M 3			L	41	54	25	
				C	41	55	24	
				Z	40	55	—	
	M 4	EH36	38	L	37	57	29	
				C	38	56	24	
				Z	40	53	—	
KTR	K 1	38	L	43	52	32		
			C	44	54	30		
			Z	43	52	33		
	K 2	EH36	35	L	43	53	28	
				C	42	53	28	
				Z	38	53	24	
	K 3			L	40	52	32	
				C	43	53	30	
				Z	38	51	21	
Convent.	C 1	SM50	35	L	32	53	39	
				C	30	53	40	
	C 2				Z	35	54	21
					L	35	53	37
					C	35	53	37
					Z	37	53	19

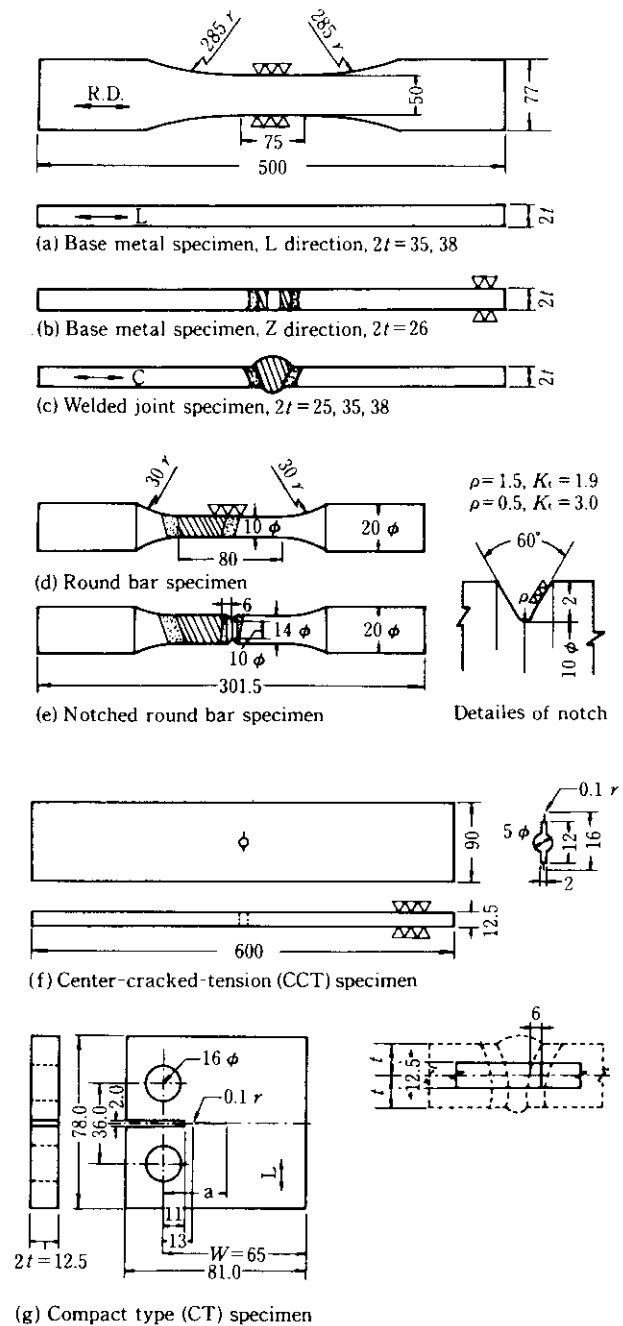


**Fig. 2** Dimension of test specimens (mm)

was prepared in the most softened part of the HAZ 6 mm from the cross bond.

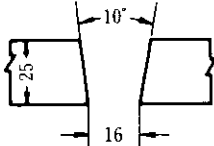
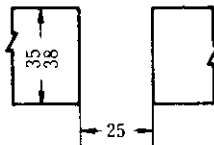
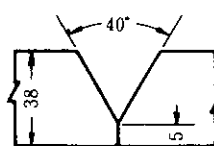
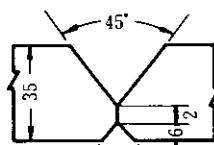
### 2.3 Experimental Procedure

The fatigue test was conducted using a  $\pm 100$ -t servo-hydraulic fatigue testing machine for flat-plate specimens and a  $\pm 10$ -t unit for round-bar specimens under load-controlled zero-to-tension at frequencies of 5 to 15 Hz. The fatigue crack propagation test was carried out using a  $\pm 50$ -t servo-hydraulic fatigue testing

machine for CCT specimens and a  $\pm 5$ -t unit for CT specimens at a stress ratio  $R$  (minimum stress/maximum stress) of 0.04. The crack length was measured with a crack gauge. The frequency used was 10 Hz. The range of stress intensity factor,  $\Delta K$ , of CCT and CT specimens was calculated by Eqs. (2)<sup>3)</sup> and (3),<sup>4)</sup> respectively. Results of the calculations were rearranged by Eq. (4).<sup>5)</sup>

$$\text{CCT: } \Delta K = \sigma_R \cdot \sqrt{\pi a} \cdot \sqrt{W/\pi a \tan(\pi a/W)} \quad \dots \dots \dots (2)$$

Table 3 High heat input welding conditions

Process	Steel	Welding method	Shape of groove	Welding current (A)	Arc voltage (V)	Travel speed (cm/min)	Heat input (kJ/cm)
MACS	M 1	EG		660	30	7.2	165
	M 2	CES		500	40	1.9	632
	M 3			510	32	2.0	490
MACS	M 4	One side welding (OSW)		1 450	33	38	266
KTR	K 1			1 350	42		
KTR	K 3	ditto		1 350	36	25	229
Conven.	C 1			1 000	47		

$$CT: \Delta K = \frac{\Delta P}{2t\sqrt{W}} \cdot \frac{(2 + a/W)}{(1 - a/W)^{3/2}} \cdot \{0.886 + 4.64(a/W) - 13.32(a/W)^2 + 14.72(a/W)^3 - 5.6(a/W)^4\} \dots (3)$$

$$\frac{da}{dN} = C(\Delta K)^m \dots (4)$$

where

- $\sigma_R$ : Stress range
- $\Delta P$ : Load range
- $a$ : Crack length
- $W$ : Specimen width
- $2t$ : Plate thickness
- $N$ : Number of cycles
- $C, m$ : Material constants

The Vickers hardness of high-heat-input welded joints was measured at a point 2 mm under the surface. Before the test, a total of eight areas in weld toes at ends of both upper and lower surfaces of all joint test specimens were enlarged tenfold by a projector and the notch radius  $\rho$ , flank angle  $\theta$ , and reinforcement height  $h$

defined in Fig. 3 were measured. The stress concentration factor,  $K_t$ , was determined from measurement results using Eq. (5)<sup>6)</sup> and the relationship between  $K_t$  and fatigue strength was investigated.

$$K_t = 1 + \left[ \frac{1 - e^{-0.9\sqrt{T/h}(\pi - \theta)}}{1 - e^{-0.9\sqrt{T/h}\pi/2}} \right] \cdot \left( \frac{1}{2.8T/t - 2} \cdot \frac{h}{\rho} \right)^{0.65} \dots (5)$$

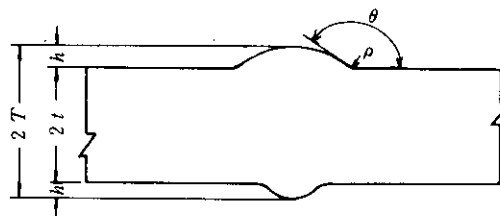


Fig. 3 Definition of the toe radius  $\rho$  and the flank angle  $\theta$

where

- $K_t$ : Stress concentration factor
- $\rho$ : Notch radius
- $\theta$ : Flank angle
- $h$ : Reinforcement height
- $2T$ : Plate thickness +  $2h$
- $2t$ : Plate thickness

### 3 Test Results

#### 3.1 Tensile Strength of High-Heat-Input Welded Joints

Table 4 shows results of the NKU2A type joint tensile

Table 4 Tensile properties of high heat input welding joints

Process	Steel		Plate thickness (mm)	Welding method	NKU2A type		HAZ tensile strength	
					TS (kgf/mm <sup>2</sup> )	Fractured location*	TS (kgf/mm <sup>2</sup> )	ΔTS** (kgf/mm <sup>2</sup> )
MACS	M 1	AH36	25	EG	52.4	BM	51	0
	M 2		35	CES	51.5	BM	50	-6
	M 3		53.0	HAZ	—	—		
	M 4	EH36	38	OSW	53.3	BM	49	-8
KTR	K 1	EH36	38	OSW	54.2	BM	51	-1
	K 3		35		53.7	BM	56	+3
Convent.	C 1	SM50	35	OSW	56.4	BM	58	+5

\* BM: Base metal  
HAZ: Heat affected zone  
\*\* BM tensile strength - HAZ tensile strength

Table 5 Results of hardness in high heat input welding joints

Process	Steel		Plate thickness (mm)	Welding method	Weld metal hardness (average)	HAZ hardness	Softening zone width (mm)	ΔHv*
MACS	M 1	AH36	25	EG	192	136	11	23
	M 2		35	CES	183	137	11	13
	M 3		180	134	25	26		
	M 4	EH36	38	OSW	202	138	10	32
KTR	K 1	EH36	38	OSW	200	153	7	11
	K 2		35		188	152	5	11
	K 3		215		155	10	19	
Conven.	C 1	SM50	35	OSW	195	151	7	+1

\* BM hardness - HAZ hardness

test and HAZ tensile test conducted on each type of steel. In the joint tensile test, specimens almost always fractured in the base metal, and the increase in strength was small. In the HAZ tensile test, however, a maximum decrease in strength of 8 kgf/mm<sup>2</sup> (78 MPa) was observed.

#### 3.2 Hardness of High-Heat-Input Welded Joints

Table 5 gives the hardness of the most softened part of the HAZ and the width of the softened part as determined from the Vickers hardness distribution of high-heat-input welded joint sections. The hardness of the most softened part of the HAZ is about 136 HV in the MACS steels and about 153 HV in the KTR steels. Therefore, the degree of softening is higher in the MACS steels than in the KTR steels. The width of the softened part also tends to be larger in the MACS steels.

#### 3.3 Geometry of High-Heat-Input Weld Toes

Table 6 shows results of measurement of weld toe geometry and of calculation of  $K_t$  for each welded joint. The  $K_t$  of low-heat-input welded joints is often 3 to 4, while that of high-heat-input welded joints is smaller. This suggests that the fatigue strength of high-heat-input welded joints can be high.

Table 6 Toe radius  $\rho$ , flank angle  $\theta$ , reinforcement height  $h$  and stress concentration factor  $K_t$  at the toe of high heat input welding joint for various high tensile strength

Process	Steel		Plate thickness (mm)	Welding method	$\rho$ (mm)	$\bar{\theta}$ (deg)	$\bar{h}$ (mm)	$K_t$
MACS	M 1	AH36	25	EG	3.20	145.9	0.91	1.39
	M 2		35	CES	1.08	136.6	2.04	2.24
	M 3		2.27	143.5	2.15	1.74		
	M 4	EH36	38	OSW	0.95	123.3	1.89	2.43
KTR	K 1	EH36	38	OSW	2.65	136.3	2.30	1.74
	K 3		35		1.04	119.7	2.80	2.55
Convent.	C 1	SM50	35	OSW	0.57	141.2	3.80	3.16

### 3.4 Fatigue Test Results

#### 3.4.1 Fatigue strength of base metal and welded joints

Figures 4, 5 and 6 summarize  $S-N$  diagrams obtained from fatigue tests conducted on specimens taken in the L- and Z-directions of base metal and high-heat-input welded joint specimens. The fatigue strength at  $2 \times 10^6$  cycles,  $\sigma_{WB}$ , obtained in L-direction base

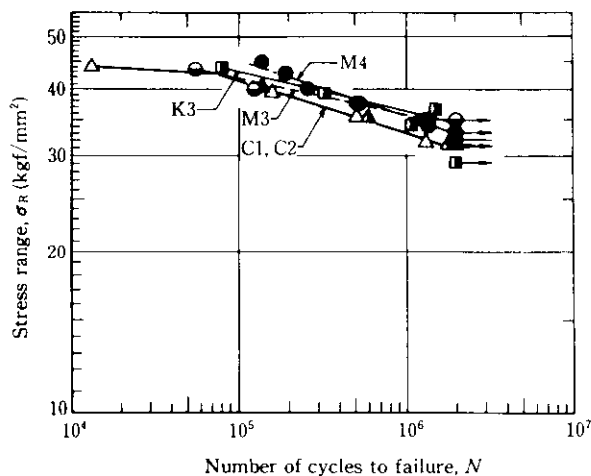


Fig. 4 S-N diagram of the base metal for MACS, KTR and conventional steels (L-direction)

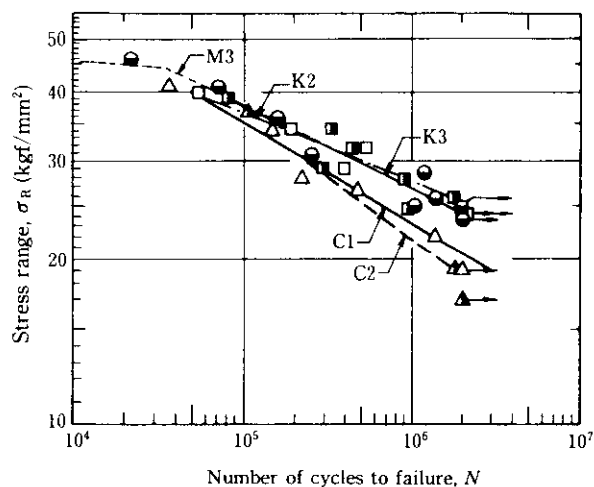


Fig. 5 S-N diagram of through-thickness specimens of MACS, KTR and conventional steels

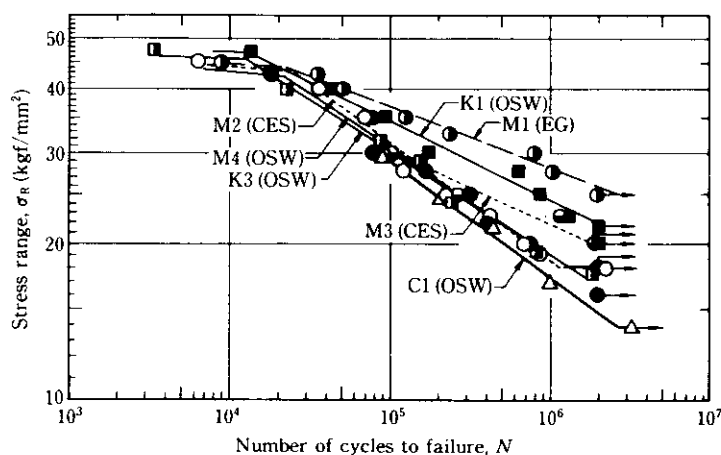


Fig. 6 S-N diagram of high heat input welded joints of MACS, KTR and conventional steels

metal specimens of MACS and KTR steels, ranges from 33 to 35 kgf/mm<sup>2</sup> (324 to 343 MPa); that of conventional steels is 31 kgf/mm<sup>2</sup> (304 MPa).

The fatigue strength at  $2 \times 10^6$  cycles,  $\sigma_{WZ}$ , obtained in Z-direction base metal specimens of MACS and KTR steels ranges from 24 to 25 kgf/mm<sup>2</sup> (235 to 245 MPa); with conventional steels the range is 18.4 to 20.4 kgf/mm<sup>2</sup> (180 to 200 MPa). There is scarcely any difference in fatigue strength between the MACS and KTR steels. These steels show fatigue strength values 4 to 5 kgf/mm<sup>2</sup> (39 to 49 MPa) higher than those of conventional steels. However, these differences in fatigue strength in the short-life region ( $N < 10^5$ ) are relatively small. In the conventional steels, the fatigue strength in the long-life region is higher with steel C 1 than with steel C 2, the sulfur content of which is higher than that of C 1. As will be described later, this difference can be understood to be caused by the difference in the sulfur content.

The fatigue strength at  $2 \times 10^6$  cycles,  $\sigma_{WJ}$ , obtained in welded joints of MACS and KTR steels ranges considerably, from 18 to 25 kgf/mm<sup>2</sup> (177 to 245 MPa). The value of  $\sigma_{WJ}$  is 25 kgf/mm<sup>2</sup> (245 MPa), the highest value, in electroslag welded joints (steel M 1). A relatively low value of 18 kgf/mm<sup>2</sup> (177 MPa) is observed in one-side welded (OSW) joints (steels M 4 and K 3) and consumable electroslag welded (CES) joints. However, the relationships between the magnitude of fatigue strength and manufacturing processes, steel grades and welding methods are not always constant. Incidentally, the  $\sigma_{WJ}$  of joints of conventional steels is 14 kgf/mm<sup>2</sup> (137 MPa).

#### 3.4.2 Fatigue strength of softened part of HAZ

For steels M4 (OSW joint) and M3 (CES joint) of MACS steel, which show great differences in hardness between the base metal and the HAZ, as in Table 5, the fatigue strength of the softened part of the HAZ was

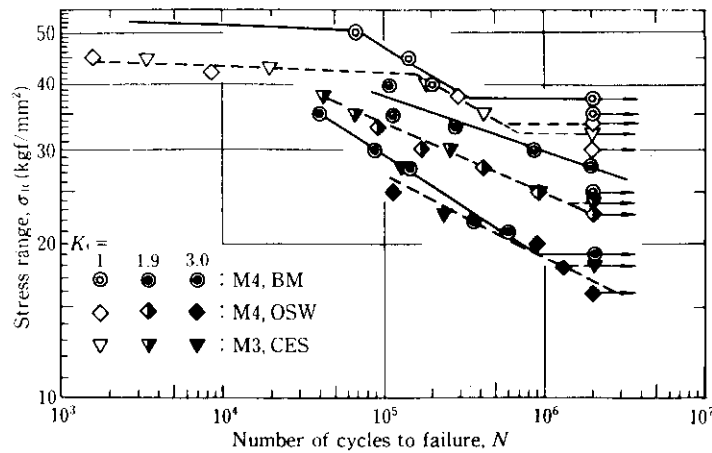


Fig. 7 *S-N* diagram of notched round bar specimens which are machined out from HAZ

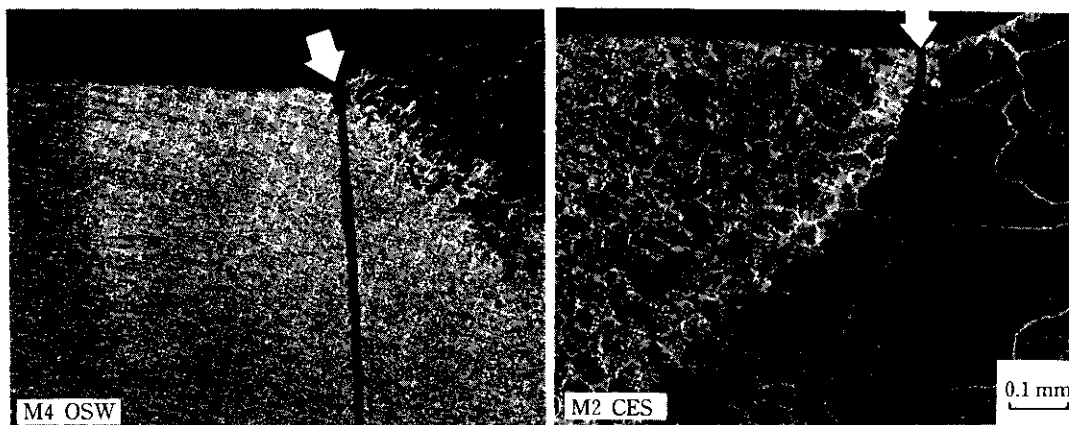


Photo 1 Fatigue crack path in high heat input welded joints (Arrow indicates crack initiation point.)

determined using the smooth and notched specimens shown in Fig. 2(d) and (e). Figure 7 is an *S-N* diagram thus obtained. This figure also shows, for comparison, the fatigue strength obtained in smooth and notched specimens of the base metal of M 4. The difference in fatigue strength between the base metal and the most softened part of the HAZ is 3 to 5 kgf/mm<sup>2</sup> (29 to 491 MPa) at  $K_t = 1$ , about 4 kgf/mm<sup>2</sup> (39 MPa) at  $K_t = 1.9$ , and 1 to 2 kgf/mm<sup>2</sup> (20 MPa) at  $K_t = 3$ . Further, the fatigue strength of the most softened part of the HAZ is lower than that of the base metal. However, this difference decreases with increasing  $K_t$ . The ratio of the fatigue strength of the HAZ to the fatigue strength of the base metal varies slightly, depending on  $K_t$  and life, ranging from 84 to 100%. If  $K_t = 3$ , this ratio is 90% or more.

### 3.4.3 Appearance of fatigue fracture

As shown in Photo 1, all fatigue fractures in welded joint specimens are observed in the weld toe, not in the

most softened part of the HAZ. Photo 2 shows the appearance of fractures in through-thickness fatigue specimens. In all cases, the fracture occurred in the test plate. The results of observation under an electron microscope are shown in Photo 3 and reveal that inclusions are present at these fatigue crack initiation points. These inclusions were analyzed by an EPMA and it was found that they are MnS and Al<sub>2</sub>O<sub>3</sub>. This suggests that inclusions have a significant effect on through-thickness fatigue properties.

## 3.5 Fatigue Crack Propagation Test

### 3.5.1 Crack propagation test of base metal

Figures 8 and 9 show the fatigue crack propagation properties observed in base metal specimens of MACS, KTR and conventional steels taken in the L-direction and through-thickness direction. CCT specimens were used to investigate the MACS steel (M 4), and CT specimens were used for all other tests. Table 7 shows



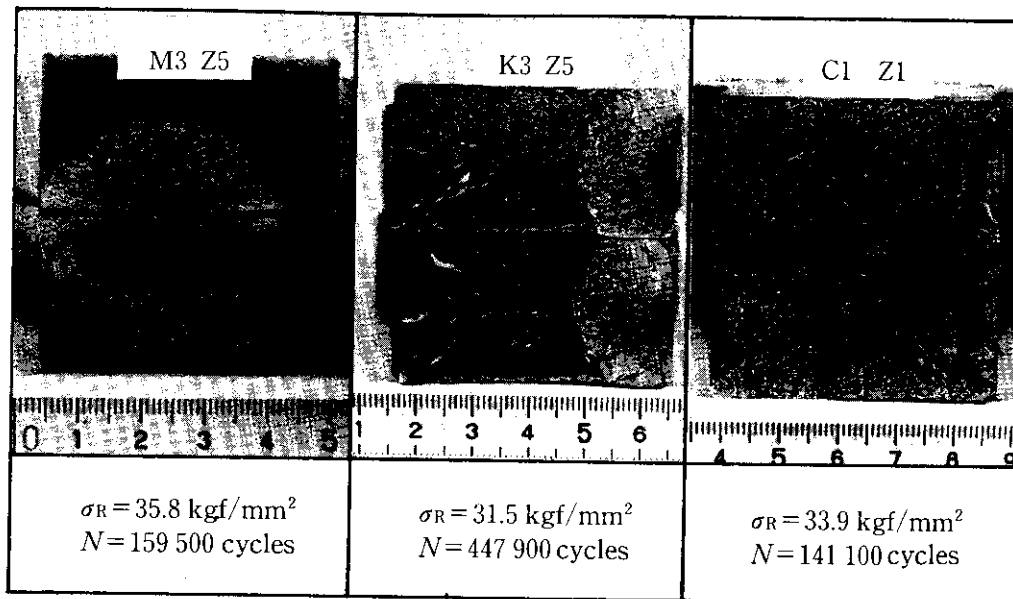


Photo 2 Fracture appearance of through-thickness fatigue specimens

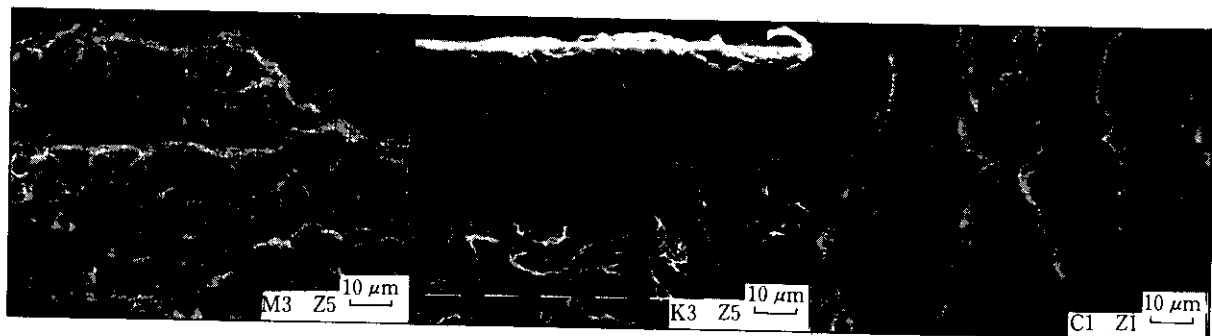


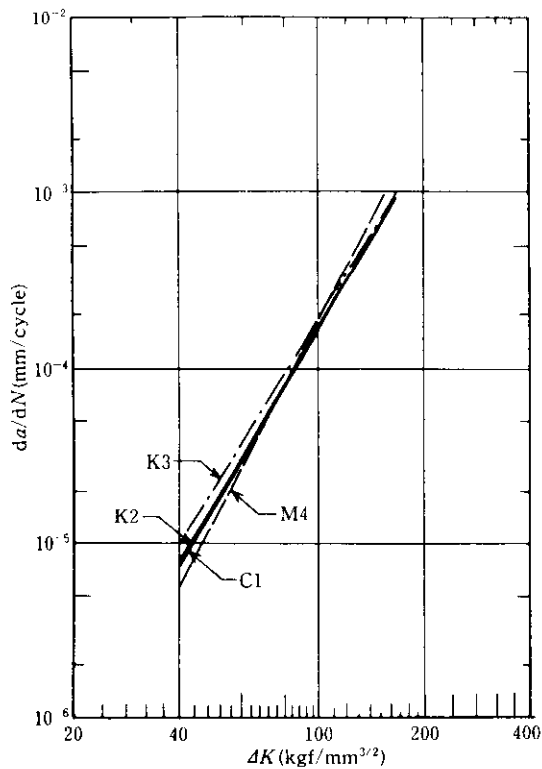
Photo 3 Scanning electronmicrographs of fatigue crack initiation point of through thickness fatigue specimens to various steels

Table 7 The value of  $m$  and  $C$  obtained in fatigue crack propagation tests

Process	Steel	L direction		Z direction		HAZ	
		$m$	$C$	$m$	$C$	$m$	$C$
MACS*	M 1	—	—	—	—	3.20	$9.91 \times 10^{-11}$
	M 2	—	—	—	—	3.24	$8.05 \times 10^{-11}$
	M 4	3.77	$5.31 \times 10^{-12}$	2.90	$2.11 \times 10^{-10}$	3.76	$7.18 \times 10^{-12}$
KTR**	K 1	—	—	—	—	3.35	$6.54 \times 10^{-11}$
	K 2	3.31	$3.88 \times 10^{-11}$	2.68	$9.85 \times 10^{-10}$	4.49	$1.14 \times 10^{-13}$
	K 3	3.20	$7.37 \times 10^{-11}$	2.93	$2.38 \times 10^{-10}$	4.52	$1.00 \times 10^{-13}$
Convent.**	C 1	3.38	$2.78 \times 10^{-11}$	3.02	$1.66 \times 10^{-10}$	4.16	$6.01 \times 10^{-13}$
	C 2	—	—	3.52	$2.26 \times 10^{-11}$	—	—

\* CCT specimen

\*\* CT specimen



**Fig. 8** Relationship between fatigue crack propagation rate,  $da/dN$ , and the range of stress intensity factor,  $\Delta K$ , in base metals of MACS, KTR and conventional steels (L-direction)

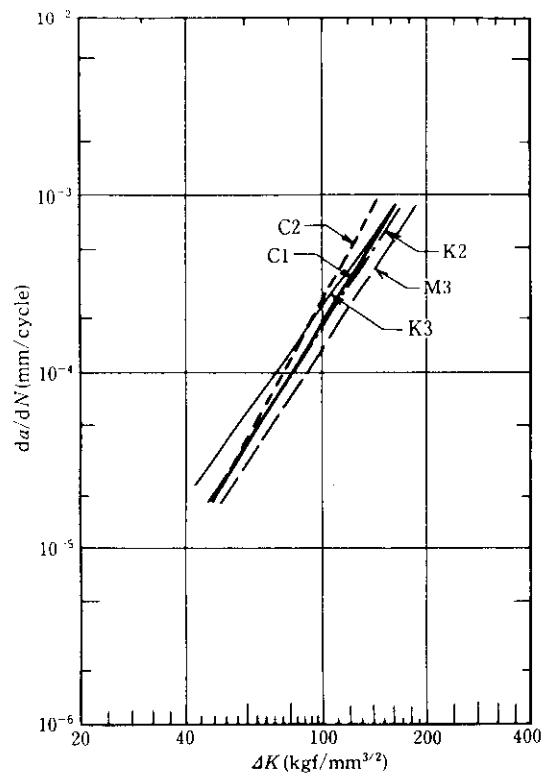


**Fig. 9** Relationship between fatigue propagation rate,  $da/dN$ , and the range of stress intensity factor,  $\Delta K$ , in through-thickness specimens of MACS, KTR and conventional steels

values of  $m$  and  $C$  of each steel as determined from the results shown in Figs. 8 and 9. Figure 9 indicates that there is no difference in the crack propagation properties in the L-direction among the MACS, KTR, and conventional steels: The crack propagation properties of these steels in the L-direction can be considered to be the same. Figure 9 shows that there are some variations in the fatigue crack propagation rate in specimens taken in the through-thickness direction. It may be said, however, that the MACS and KTR steels have resistance to fatigue crack propagation equal or superior to that of the conventional steels. The fatigue crack propagation rate of steel C 2 with a high sulfur content is higher than those of other steels, and this tendency is remarkable in the high- $\Delta K$  region. It is known that the  $m$ -value increases with increasing sulfur content<sup>7)</sup>, and the same tendency is observed.

### 3.5.2 Crack propagation properties of HAZ of high-heat-input welded joints

Figure 10 shows the crack propagation properties of the HAZ of high-heat-input welded joints of MACS, KTR and conventional steels. CCT specimens were used for the MACS steels (M 1, M 2 and M 4) and KTR steel (K 1), and CT specimens for other steels. Table 7

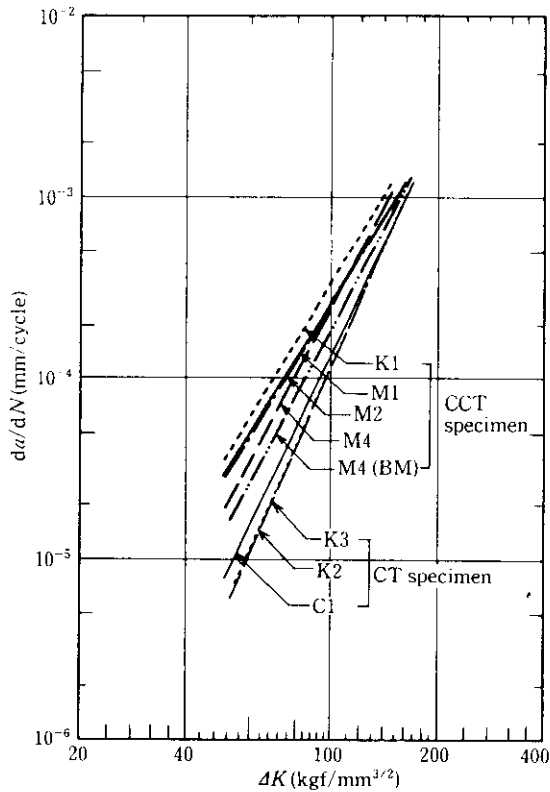
shows values of  $m$  and  $C$  of each steel as determined from this figure. Fatigue crack propagation rates obtained in the CCT specimens are higher than those of the base metal specimens, while fatigue crack propagation rates obtained in the CT specimens are lower than those of the base metal specimens. It is considered that this is because residual tensile stresses act on the area near the crack tip of a CCT specimen, but residual compressive stresses act in a CT specimen.<sup>8)</sup> A comparison of results obtained from the same specimen reveals that there is no difference caused by the difference in manufacturing processes.

## 4 Discussion

### 4.1 Fatigue Strength

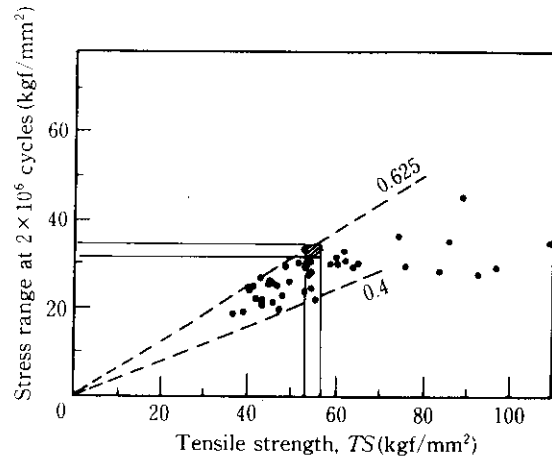
#### 4.1.1 Comparison between TMCP and conventional steels

Figure 11 summarizes the S-N diagram of base metal specimens (L-direction) and welded joint specimens of MACS, KTR, and conventional steels. This figure contains past data<sup>9)</sup> for reference. The  $\sigma_{WB}$  of the base metal of TMCP steels ranges from 33 to 35 kgf/mm<sup>2</sup> (324 to 343 MPa); that of the base metal of conven-



**Fig. 10** Relationship between fatigue crack propagation rate,  $da/dN$ , and the range of stress intensity factor,  $\Delta K$ , in high heat input welded joints (HAZ) of MACS, KTR and conventional steels

tional steels (C 1 and C 2) and SM50B in past data is  $31 \text{ kgf/mm}^2$  (304 MPa). In Fig. 12, the relationship between  $\sigma_{WB}$  and tensile strength is included in past



**Fig. 12** Correlation between tensile strength and fatigue strength of base plates with mill scale on the specimens surface

data.<sup>10)</sup> The values of TMCP steels are close to the upper limit of the variation range of base metal with mill scale shown in past data. Therefore, it may be said that the fatigue strength of the base metal of TMCP steels is equal or superior to that of the conventional steels.

The fatigue strength of welded joints of TMCP steels ranges considerably, from 18 to 25  $\text{kgf/mm}^2$  (177 to 245 MPa). However, these values of fatigue strength are higher than the value obtained in OSW joints of conventional steel C 1 ( $\sigma_{wJ}$  of  $14.6 \text{ kgf/mm}^2$ ) (143 MPa) and are distributed in a range from the middle to above the upper limit of the range<sup>9)</sup> shown by past data obtained in SAW joints of SM50B. It may be said that the fatigue strength of high-heat-input welded joints of TMCP steels is equal or superior to that of welded joints of the

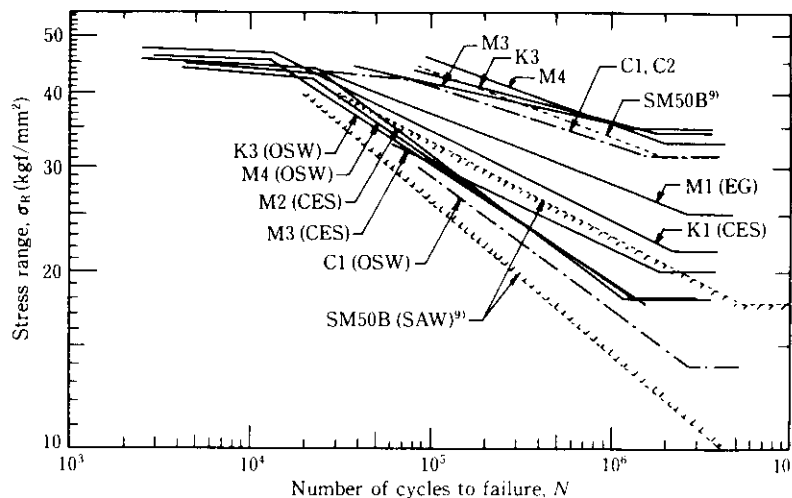


**Fig. 11**  $S-N$  diagram of base metals and high heat input welded joints of MACS, KTR and conventional steels

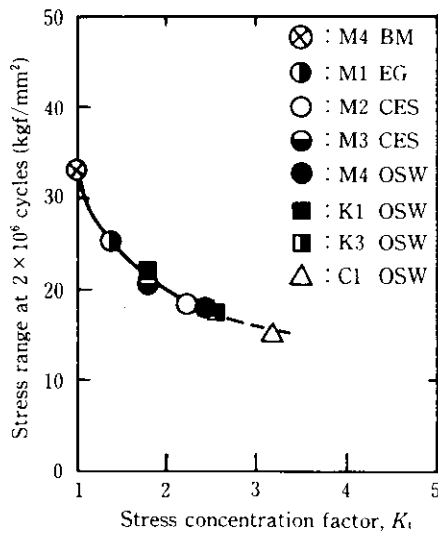


**Fig. 13** Relationship between stress range at  $2 \times 10^6$  cycles and stress concentration factor,  $K_t$ , in high heat input welded joints

conventional steels.

#### 4.1.2 Effect of weld toe geometry

As is apparent from Photo 1, fatigue cracks almost always form in the weld toe in the fatigue test on welded joints. Stresses are concentrated in the weld toe, and it is evident that  $K_t$  has a significant effect. **Figure 13** shows the relationship between the fatigue strength of welded joints and  $K_t$  (Table 6). A steel showing high fatigue strength in Fig. 11 shows a low  $K_t$ -value of 1.4, with a steel relatively low in fatigue strength showing a high  $K_t$ -value of 2.4. The  $K_t$  of a conventional steel is as high as 3.4, which is the highest value among the high-heat-input welded joints. Therefore, it might be thought that the difference in the fatigue strength of welded joints is caused by the difference in the weld toe geometry.

#### 4.1.3 Softening in HAZ and fatigue strength

The tensile strength of M 4, which had the lowest strength in the HAZ tensile test as shown in Table 4, is  $49 \text{ kgf/mm}^2$  ( $481 \text{ MPa}$ ), about  $8 \text{ kgf/mm}^2$  ( $78 \text{ MPa}$ ) lower than the strength of the base metal. Table 5 shows that the hardness of the softened part of the HAZ of M 4 is also lower by 32 HV than the base metal. This decrease virtually corresponds to the decrease in tensile strength. Therefore, the amount of softening in the HAZ of the test material may be considered to be a maximum of  $8 \text{ kgf/mm}^2$  ( $78 \text{ MPa}$ ). An investigation was made into the degree of the effect of softening of this order on fatigue strength. It should be noted, however, that as mentioned above, fatigue cracks almost always develop in the weld toe, where there is less softening than in the softened part of the HAZ and, as well, some-

**Table 8** Comparison of measured and calculated fatigue strength, reduction due to softening of HAZ various stress concentration factor,  $K_t$

Stress concentration factor, $K_t$	1.0	1.9	3.0
Cal. $\Delta\sigma_{wn}$ ( $\text{kgf/mm}^2$ )	4.8	2.5	1.6
Meas. $\Delta\sigma_{wn}$ ( $\text{kgf/mm}^2$ )	3~5	$\approx 4.0$	1~2

times more hardening than in the base metal.

If a welded joint is regarded as a kind of notched specimen, its fatigue strength  $\sigma_{wn}$  can be estimated from the fatigue strength of the base metal,  $\sigma_{wb}$ , and the  $K_t$  of the weld toe. Because  $\sigma_{wb}$  is considered to be generally proportional to tensile strength, it is given by Eq. (6):

$$\sigma_{wb} = \alpha \cdot TS \dots\dots\dots (6)$$

Where  $\alpha$  is a proportionality constant and is approximately 0.6 in the case of fatigue strength under zero-to-tension loading. as a first approximation,  $\sigma_{wn}$  is given by Eq. (7), if notch sensitivity is not considered:

$$\sigma_{wn} = \sigma_{wb}/K_t \dots\dots\dots (7)$$

Hence Eq. (8) is obtained from Eqs. (6) and (7):

$$\sigma_{wn} = \alpha \cdot TS/K_t \dots\dots\dots (8)$$

Now, if the change in  $\sigma_{wn}$ , which occurs when  $TS$  changes by  $\Delta TS$ , is supposed to be  $\Delta\sigma_{wn}$ , then:

$$\Delta\sigma_{wn} = \alpha \cdot \Delta TS/K_t \dots\dots\dots (9)$$

The relationship between a change in fatigue strength,  $\Delta\sigma_{wn}$ , of a welded joint and  $K_t$  was determined for a case where  $\Delta TS$  was taken as  $8 \text{ kgf/mm}^2$  ( $78 \text{ MPa}$ ) and  $\alpha$  as 0.6, as mentioned above. **Table 8** gives results of the calculation. This table also shows results of experiment with round-bar specimens. The calculation results are in good agreement with the experimental results. It may be said from this that the effect of softening is significant when the weld toe has a smooth geometry and  $K_t$  is small (in this case, the value of fatigue strength is high) and that the effect of softening decreases with increasing  $K_t$ . It may be thought that the effect of softening in the HAZ is negligibly small because stress concentration occurs in actual welded joints and the softening at crack initiation points is slight.

#### 4.1.4 Comparison between fatigue strength in through-thickness direction and that in L-direction

**Figure 14** shows the relationship between the ratio of the fatigue strength in the through-thickness direction to fatigue strength in the L-direction,  $\sigma_{wz}/\sigma_{wL}$ , and the sulfur content, together with past data<sup>7)</sup>. This fatigue

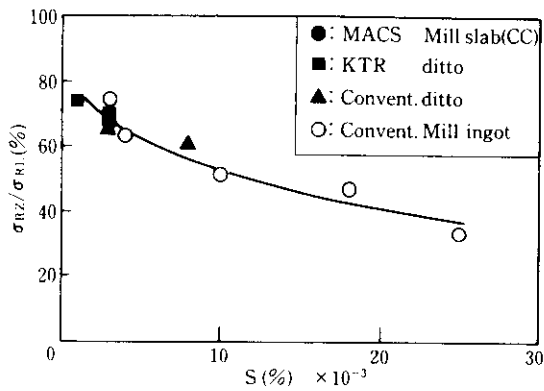


Fig. 14 Variation of fatigue strength ratio in through-thickness direction,  $\sigma_{wZ}/\sigma_{wL}$ , with sulfur content in MACS, KTR and conventional steels

strength ratio is approximately 70% in the TMCP steels and approximately 63% in the conventional steels. Figure 14 clearly shows that the  $\sigma_{wZ}/\sigma_{wL}$  ratio tends to increase with decreasing sulfur content. The relationship between the rate of decrease in through-thickness fatigue strength and the sulfur content observed in the TMCP steels is the same as the relationship in the conventional steels. This relationship can be understood in terms of the effect of inclusions.

## 4.2 Fatigue Crack Propagation

### 4.2.1 Comparison between TMCP steels and conventional steels

Many investigators<sup>11)</sup> have shown that the relationship given by Eq. (10) exists in Paris' formula between

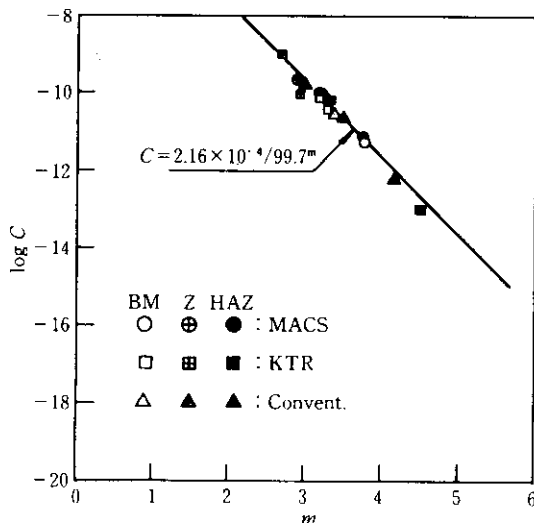


Fig. 15 Correlation between  $m$  and  $\log C$  in Paris' formula

the material constant  $C$  and  $m$ , and that this equation holds for steels ranging from mild steels to high-strength steels.

$$C = A/B^m \dots \dots \dots (10)$$

According to a report<sup>12)</sup>,  $A = 2.14 \times 10^{-4}$  and  $B = 99.7$ . Figure 15 shows this relationship together with the results of experiments with the present TMCP steels and conventional steels. Results obtained from the base metal and welded joints of TMCP steels also agree with an equation shown in the above-mentioned report.<sup>12)</sup>

### 4.2.2 Softening in HAZ and fatigue-crack propagation rate

It has been confirmed that the relationship given by Eq. (11) exists between the material constant  $m$  and the yield stress  $YP$ :

$$m = m_0 - \beta \cdot YP \dots \dots \dots (11)$$

Although investigators have shown various values of  $m_0$  and  $\beta$ ,  $m_0 = 4.7$  and  $\beta = 0.035$  or so if the averages of values shown in many data are taken. According to Table 4, the difference in tensile strength between the base metal and the softened part of the HAZ is a maximum 8 kgf/mm<sup>2</sup> (78 MPa). This value is approximately 5 kgf/mm<sup>2</sup> (49 MPa) when converted to  $YP$ . If this converted value is considered to be the minimum  $YP$ , the change in  $m$  is only about 0.175 (= 0.2), an almost negligible difference. By substituting Eq. (10) showing the relationship between  $C$  and  $m$  for Eq. (4), a formula for crack propagation, we obtain:

$$da/dN = A \cdot (\Delta K/B)^m \dots \dots \dots (12)$$

This means that  $da/dN$  is  $A$  when  $\Delta K$  is  $B$ , irrespective of the material used. The above-mentioned values were obtained for  $A$  and  $B$ . Figure 16 shows changes in the relationship between  $da/dN$  and  $\Delta K$  resulting from the softening of the HAZ, in which the foregoing facts are taken into consideration. Changes in the relationship between the  $da/dN$  and  $\Delta K$  due to the softening of the HAZ are predictable as the differences in the solid and dotted line. These changes, however, are practically negligible.

### 4.2.3 Crack propagation rate in through-thickness direction

Figure 17 shows the relationship between  $da/dN$  and sulfur content found in specimens of TMCP and conventional steels<sup>12)</sup> in the through-thickness direction. In the conventional steels,  $da/dN$  increases when the sulfur content exceeds 0.01%. The higher the  $\Delta K$  value, the more noticeable this tendency will be. It has been reported,<sup>12)</sup> however, that this tendency is not observed in specimens taken in the L-direction. In this

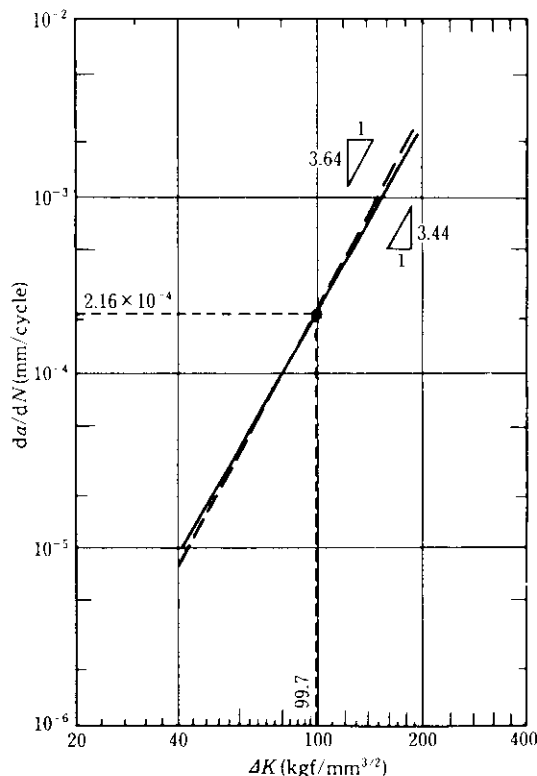


Fig. 16 Estimated influence of softening in HAZ on the fatigue crack propagation behaviour

figure, the  $da/dN$  of the specimens of TMCP steels taken in the through-thickness direction is almost on an extension of the curve for the conventional steels. Thus, no additional factor resulting from the difference in manufacturing processes can be observed.

## 5 Conclusions

Fatigue tests under zero-to-tension and fatigue crack propagation tests were conducted on base metals and high-heat-input welded joints of 50-kgf/mm<sup>2</sup> (490 MPa) high-strength steels manufactured by the TMCP processes (KTR and MACS). The following conclusions were obtained:

- (1) The fatigue strength  $\sigma_{WB}$ , at  $2 \times 10^6$  cycles of the base metal of TMCP steels ranges from 33 to 35 kgf/mm<sup>2</sup> (324 to 343 MPa). The fatigue strength ratio,  $\sigma_{WB}/TS$ , is 0.58 to 0.65 and is close to the upper limit of the range of data on the conventional steels.
- (2) The fatigue strength of high-heat-input welded joints of TMCP steels is 18 to 25 kgf/mm<sup>2</sup> (177 to 245 MPa), while that of the conventional steels is approximately 15 kgf/mm<sup>2</sup> (147 MPa). Thus, the fatigue strength of the TMCP steels is equal or superior to that of the conventional steels.
- (3) The stress concentration factor,  $K_t$ , for the weld toe is 1.39 to 3.16. The lower the  $K_t$  value, the higher

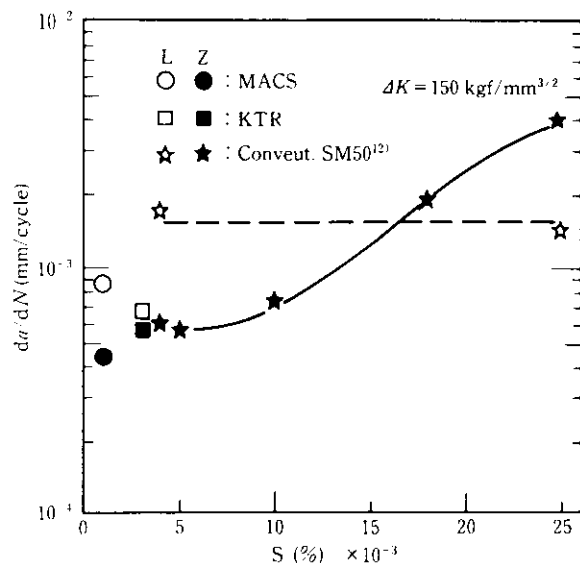


Fig. 17 Influence of sulfur content on the fatigue crack propagation rates

the fatigue strength. The difference in fatigue strength of welded joints may be considered to be the difference in  $K_t$ .

- (4) The decrease in fatigue strength due to the softening in the HAZ is estimated at approximately 5 kgf/mm<sup>2</sup> (49 MPa) for smooth specimens and 1.6 kgf/mm<sup>2</sup> (16 MPa) at  $K_t$  of 3. This result agreed with results with round-bar specimens. The effect of softening in the HAZ would be regarded as negligible in welded joints where stress concentration occurs.
- (5) The through-thickness fatigue strength increases with decreasing sulfur content. This tendency is also observed in the conventional steels and can be understood as an effect of inclusions.
- (6) The fatigue crack propagation properties of the TMCP steels, observed both in the base metal and welded joints, were in good agreement with the equation obtained in the conventional steels, i.e.,  $C = 2.16 \times 10^{-4}/99.7^m$ .
- (7) The change in  $m$ , an exponent in the equation for fatigue crack propagation, resulting from softening in the HAZ is estimated at 0.2 or under and is practically negligible.
- (8) The through-thickness crack propagation rate of the TMCP steels has a correlation to the sulfur content and no additional factors resulting from the difference in manufacturing processes were observed.

## References

- 1) R. B. Heywood: "Designing by Photoelasticity", (1952), 167-187, [Chapman and Hall]

- 2) R. E. Peterson: "Stress Concentration Design Factor", (1953), [John Wiley]
- 3) P. C. Paris and G. C. Sih: ASTM STP 381, (1965), 30
- 4) ASTM E647-78T
- 5) P. C. Paris and F. Erdogan: *J Basic. Eng.*, **85**(1963), 528
- 6) M. Nishida: "Stress Concentration", (1971), [Morikita Ink.]
- 7) K. Kobayashi, A. Narumoto, T. Funakoshi and M. Hirai: *Kawasaki Steel Giho*, **8**(1976)3, 336
- 8) National Research Institute for Metals: "NRIM fatigue data sheet technical document", No. 3 (1984)
- 9) National research Institute for Metals: "NRIM fatigue data sheet", No. 27 (1981)
- 10) T. R. Gurney: "Fatigue of Welded Structure", (1968), [Cambridge University Press]
- 11) H. Kitagawa: *Trans. of the Japan Society of Mechanical Engineers*, **75**(1971)642, 1068
- 12) K. Kobayashi, A. Narumoto, M. Tanaka and T. Funakoshi: *Tetsu-to-Hagané*, **64**(1978)7, 1072